

# Multiuser Detection with Differentially Encoded Data for Mismatched Flat Rayleigh Fading CDMA Channels

by

Hsin-Yu Wu and Alexandra Duel-Hallen

Department of Electrical and Computer Engineering  
Box 7911, North Carolina State University  
Raleigh, NC 27695  
internet: hwu@eos.ncsu.edu, sasha@eos.ncsu.edu

## Abstract

In this paper, we evaluate the performance of several multiuser detectors for flat Rayleigh fading CDMA channels without perfect knowledge of fading channel coefficients. The fading channel is modeled as a second order Auto Regressive (AR) process and is estimated using a Kalman filter. Burst errors caused by phase reversal of channel estimates can be effectively resolved by using differential encoding. The Bit Error Rates (BERs) of these multiuser detectors with Kalman channel estimators are evaluated through analysis and simulations. The results show that the decorrelator is more robust than other more complex multiuser detectors.

## 1. Introduction

Multiuser detection has a potential to increase the capacity and solve the near-far problem of current CDMA systems. The performance of several suboptimal multiuser algorithms, including the linear decorrelator [1], the multi-stage detector [2], the decision-feedback detector [3], and the successive interference cancellation scheme [4], were evaluated for both Additive White Gaussian Noise (AWGN) and fading channels. However, ideal assumptions, such as perfect channel and delay estimation, were made in most of these investigations. It is important to assess the realistic performance of these detectors without such ideal assumptions. In this paper, we compare the performance of several multiuser detectors when channel mismatch is present. In particular, we concentrate on the decorrelator, the two-stage detector with the decorrelating first stage (2S), and the decision-feedback (DF) detector for mismatched Rayleigh flat fading synchronous CDMA channels.

The channel mismatch condition considered here results from generating channel estimates and replacing the channel coefficients by these estimates in the multiuser detector structure. In [5], it is shown that an AR process can be estimated using a Kalman filter. In [6], a Rayleigh fading channel is modeled as a second order AR process because their Power Spectrum Densities (PSDs) have similar spectral peak structures. Based on

the AR model, the Kalman filter can be easily implemented. The channel mismatch, characterized by the mean square estimation error, was shown to degrade the performance of multiuser detectors [7][8]. In addition, when the Kalman channel estimator operates in the decision-directed mode, deep fades may trigger "reversal phenomenon" in which the channel estimate has nearly 180 degree phase shift relative to the actual channel coefficient [9]. The reversal phenomenon causes burst errors and gives unacceptably high error rates. In this paper, we propose to use the differentially encoding scheme to avoid burst errors.

The BERs of these multiuser detectors using differentially encoding scheme was evaluated by simulations as well as analytically [7][8]. We find that the performance of the decorrelator is degraded only by the channel estimation error of the desired user whereas the performance of the 2S and the DF detectors is limited by the channel estimation errors of both the desired user and other users. The accumulation of the channel estimation errors results in performance loss of the 2S and the DF relative to the decorrelator. In addition, the 2S and the DF degrade in the near-far scenarios. These new results suggest that more complex multiuser detectors might be less robust than the decorrelator in practice.

The paper is arranged as follows: Section 2 reviews the mathematical model of the synchronous CDMA system and the structures of considered multiuser detectors. Section 3 discusses channel estimation issues and utilization of the differential encoding scheme. Section 4 provides the analysis of the Bit Error Rates of multiuser detectors with channel estimators. Several numerical examples are presented in Section 5 and the conclusion and future directions are given in Section 6.

## 2. Synchronous CDMA System Model and Multiuser Detectors

Consider a discrete-time model of a synchronous CDMA Rayleigh flat fading channel with  $N$  users. The sampled output of the matched filter bank at the receiver can be expressed by a complex column vector  $\mathbf{y}(k)$ ,

$$\mathbf{y}(k) = \mathbf{R}\mathbf{W}(k)\mathbf{b}(k) + \mathbf{n}(k), \quad (1)$$

where the column vector  $\mathbf{b}(k)$  consists of the information bits  $\{+1, -1\}$  of  $N$  users, and the  $N \times N$  matrix  $\mathbf{R}$  is the

normalized signature cross-correlation matrix whose components  $\mathbf{R}_{l,m}$  are the normalized cross-correlations between the signature waveforms of users  $l$  and  $m$ . The complex column vector  $\mathbf{n}(k)$  is an N-dimensional complex Gaussian noise vector with the covariance matrix

$\mathbf{E}(\mathbf{n}^* \mathbf{n}) = \mathbf{R} \mathbf{N}_0$  (\* denotes the conjugate transpose). The matrix  $\mathbf{W}(k)$  is the diagonal channel gain matrix. Since we consider a flat fading channel, there is only one fading path for each user, and the dimension of this matrix is  $N \times N$ . The diagonal components are  $\mathbf{W}_{n,n} = \sqrt{E_{b_n}} C_n(k)$   $= \sqrt{E_{b_n}} |C_n(k)| \exp(-j\theta_n(k))$  ( $n = 1, \dots, N$ ), where  $E_{b_n}$  is the symbol energy of user  $n$  and  $C_n(k)$  is the channel coefficient of user  $n$ . Assuming that fading is slow, we can model the channel coefficient  $|C_n(k)| \exp(-j\theta_n(k))$  as a constant during a symbol period. For Rayleigh fading channels, the channel coefficient is a zero mean, unity variance complex Gaussian random variable whose amplitude  $|C_n(k)|$  is Rayleigh distributed and whose phase  $\theta_n(k)$  is uniformly distributed on  $[0, 2\pi)$ .

The decorrelator is obtained by multiplying the output of the matched filter bank  $\mathbf{y}(k)$  in (1) by the inverse of the correlation matrix  $\mathbf{R}$  ( $\mathbf{R}$  is assumed to be nonsingular):

$$\mathbf{z}(k) = \mathbf{R}^{-1} \mathbf{y}(k) = \mathbf{W}(k) \mathbf{b}(k) + \mathbf{v}(k), \quad (2)$$

where the noise vector  $\mathbf{v}(k) = \mathbf{R}^{-1} \mathbf{n}(k)$ . The decision for the  $n$ -th user is made by  $\hat{b}_n(k) = \text{sgn}(\text{Re}[z_n(k) \hat{C}_n^*(k)])$ ,

where  $\hat{C}_n(k)$  is the estimate of the channel coefficient  $C_n(k)$ . The two-stage detector with the decorrelating first stage uses tentative decisions from the decorrelator to reconstruct the Multi-Access Interference (MAI). In the second stage, the reconstructed MAI of the  $n$ -th user is

$$MAI_n(k) = \sum_{i=1, i \neq n}^N \mathbf{R}_{n,i} \hat{\mathbf{W}}_{i,i}(k) \hat{b}_i(k),$$

where  $\hat{\mathbf{W}}_{i,i}(k) = \sqrt{E_{b_i}} \hat{C}_i(k)$ . The reconstructed MAI is then subtracted from the output of the matched filter bank (1). The final decision for the  $n$ -th user is made after canceling its interference, i.e.,

$$\hat{b}_n(k) = \text{sgn}\{\text{Re}[\{y_n(k) - MAI_n(k)\} \hat{C}_n^*(k)]\}.$$

The decision-feedback detector first arranges the users in the descending energy order. The sorted channel gain matrix  $\mathbf{W}^S(k)$  has decreasing diagonal elements, i.e.,  $|\mathbf{W}_{1,1}^S(k)| \geq |\mathbf{W}_{2,2}^S(k)| \geq \dots \geq |\mathbf{W}_{N,N}^S(k)|$  (the estimates of energies are used in the actual implementation). The entries in the cross-correlation matrix  $\mathbf{R}(k)$  are also rearranged based on this order. The cross-correlation matrix  $\mathbf{R}(k)$  is factored into  $\mathbf{R}(k) = \mathbf{F}^T(k) \mathbf{F}(k)$  by Cholesky factorization, where  $\mathbf{F}(k)$  is a left lower triangular matrix. Applying the noise-whitening filter  $(\mathbf{F}(k)^T)^{-1}$  to the sorted output of the matched filter bank gives a new output vector:

$$\hat{\mathbf{y}}(k) = \mathbf{F}(k) \mathbf{W}^S(k) \mathbf{b}^S(k) + \hat{\mathbf{u}}^S(k), \quad (3)$$

where the superscript  $s$  denotes the sorted results, and  $\hat{\mathbf{u}}^S(k)$  is white complex Gaussian noise vector with the covariance matrix  $\mathbf{N}_0 \mathbf{I}$ . The lower triangular structure of  $\mathbf{F}(k)$  indicates that the signal of each user  $\hat{y}_n(k)$  in (3) contains no interference from weaker users; it only contains the interference from stronger users. Therefore,

the strongest user (index=1), whose signal contains no interference, makes its decision first, and then feeds this decision back to the second strongest user to cancel the interference caused by the strongest user. Similarly, for the  $n$ -th strongest user, the decisions of the first  $n-1$  stronger users are used to cancel the interference, and its decision is made by

$$\hat{b}_n^k(k) = \text{sgn}\{\text{Re}[\{y_n^k(k) - \sum_{m=1}^{n-1} \mathbf{F}_{n,m}(k) \hat{\mathbf{W}}_{m,m}^S(k) \hat{b}_m^k(k)\} \hat{C}_n^{k*}(k)]\}.$$

The process continues until a decision is made for the weakest user.

### 3. Channel Estimation and Differential Encoding

Because the channel coefficient of a fading channel varies rapidly, traditional carrier recovery --Phase-Lock Loop (PLL) is not able to track the phase variation. It was suggested in [10] to replace a PLL by a Kalman filter. To use a Kalman filter as a channel estimator, we need a channel model with a rational spectrum. A second order AR process can be used to model a flat fading channel since it approximates the narrow band spectral peaks at the maximum Doppler frequencies of the power spectrum density of a Rayleigh fading channel [6]. The discrete time model of the fading coefficient for user  $n$ ,  $C_n(k)$ , is given by,

$$C_n(k) = -a_1 C_n(k-1) - a_2 C_n(k-2) + w(k), \quad (4)$$

where  $w(k)$  is the driving noise of the fading process, and  $a_1$  and  $a_2$  are the parameters of the AR process, which are determined by the maximum Doppler frequency  $f_d$ , the sampling period  $T$ , and the radius of the pole locations of (4). The measurement or the observation used to estimate the channel coefficient of user  $n$  is the output of the decorrelator for user  $n$ ,

$$\begin{aligned} z_n(k) &= \sqrt{E_{b_n}} b_n(k) C_n(k) + v_n(k) \\ &= \mathbf{H}_n^T(k) \mathbf{X}_n(k) + v_n(k), \end{aligned} \quad (5)$$

where  $\mathbf{H}_n(k) = \sqrt{E_{b_n}} b_n(k) [1 \ 0]^T$ , and  $v(k)$  is the Gaussian noise at the  $n$ -th output of the decorrelator with variance  $\mathbf{N}_0 [\mathbf{R}^{-1}]_{n,n}$ . With the fading model (4) and the measurement (5), the channel estimate can be generated by a Kalman filter [5],

$$\hat{\mathbf{X}}_n(k+1) = [\mathbf{A} - \mathbf{K}_n(k) \mathbf{H}_n^T(k)] \hat{\mathbf{X}}_n(k) + \mathbf{K}_n(k) z_n(k), \quad (6)$$

where the column vector  $\hat{\mathbf{X}}_n(k) = [\hat{C}_n^s(k) \ \hat{C}_n^s(k-1)]^T$  is

the channel estimate vector, the matrix  $\mathbf{A} = \begin{bmatrix} -a_1 & -a_2 \\ 1 & 0 \end{bmatrix}$ ,

and the matrix  $\mathbf{K}_n(k)$  is the Kalman filter gain obtained recursively from Ricatti equation [5]. The whole receiver structure consists of a multiuser detector for  $N$  users and  $N$  Kalman filters.

In the decision-directed mode, where  $\mathbf{H}_n(k)$  in (6) is replaced by  $\hat{\mathbf{H}}_n(k) = \sqrt{E_{b_n}} \hat{b}_n^s(k) [1 \ 0]^T$ , the channel estimate  $\hat{C}_n^s(k)$  sometimes appears to have nearly 180 degrees phase shift relative to the channel coefficient  $C_n(k)$ . The effect is denoted as "reversal phenomenon," and is shown in Figure 1. The reversal is triggered by several consecutive decision errors when the channel undergoes a deep fade. The mathematical derivation of the

causes of the reversal phenomenon can be found in [9]. Once the reversal is established, it will cause burst errors and raise the BER to the range of  $10^{-1}$ . In [9], we proposed to use an ARQ scheme with threshold detection to avoid these catastrophic events, but the scheme is not practical because of the problems arising in the threshold level selection, low throughputs, and increased delays. A more realistic and efficient solution is to encode the data bits differentially. The data bits  $b(k)$  are encoded as phase differences between transmitted bits  $a(k)$ , i.e.,  $a(k) = b(k) \oplus a(k-1)$ , where  $\oplus$  is addition mod-2 (exclusive OR). The data bit  $b(k)$  can be recovered by  $b(k) = a(k) \oplus a(k-1)$  at the receiver. It can be easily verified that burst errors can be avoided by using differential encoding. During the reversal, although phases of most decisions are shifted by  $\pi$  from the transmitted bits, most of the differences between the consecutive transmitted bits are not changed. Therefore, the data bits encoded as the differences between the consecutive transmitted bits should be preserved in the reversal interval. The errors occur only at the beginning and the end of the reversal or are sparsely scattered within the reversal interval.

Both coherent and noncoherent detection can be applied to demodulate differentially encoded data [11]. We denote coherent detection by Differentially Coherent PSK, or DC-PSK, and noncoherent detection by Differential PSK, or DPSK. Noncoherent reception (DPSK), which requires no channel estimation, is much simpler and is widely used in communications for fading channels; however, its performance is usually poorer than that of coherent reception. Furthermore, among multiuser detectors considered in this paper, the use of DPSK is limited to the decorrelator [12]. The reason is that the output of the decorrelator is identical to that of a single user system with enhanced noise. The decision process does not involve interference reconstruction. Therefore, channel estimates are not required, and noncoherent detection can be applied. On the other hand, for the 2S and the DF detectors, or any other MAI canceling type multiuser detector, coherent detection (DC-PSK) is necessary since channel estimation must be performed in order to reconstruct and cancel MAI.

#### 4. BER Analysis

To obtain the BERs of multiuser detectors using DC-PSK, we first study the BER of BPSK since the relation of BER of the DC-PSK and BER of the BPSK is given by (assuming that the decisions of each data bits are independent),

$$PE_{DC-PSK} = 2 (1 - PE_{BPSK}) PE_{BPSK}. \quad (7)$$

In the decision-directed mode, the decision of the current bit affects the channel estimate of the next bit and therefore affects the decision of the next bit. However, when SNR is high enough, occurrence of the reversal is highly reduced, and (7) is an accurate approximation. The BER and the lower bound on BER of BPSK of the three detectors are given by following expressions. Decorrelator [7]:

$$PE_{dec,BPSK} = \frac{1}{2} \left[ 1 - \sqrt{\frac{1 - \Gamma_1}{1 + [\mathbf{R}^{-1}]_{1,1} / \bar{\gamma}_1}} \right], \quad (8)$$

Two-stage detector [8]:

$$PE_{2S,BPSK} \geq \frac{1}{2} \left[ 1 - \sqrt{\frac{1 - \Gamma_1}{1 + \sum_{i=2}^N (Eb_i / Eb_1) [\mathbf{R}_{1,i}]^2 \Gamma_i + 1 / \bar{\gamma}_1}} \right], \quad (9)$$

Decision-Feedback Detector [8]:

$$PE_{DF,BPSK} \geq \frac{1}{2} \left[ 1 - \sqrt{\frac{1 - \Gamma_1}{1 + \sum_{i=1}^{N-1} (Eb_i^s / Eb_1) [\mathbf{R}_{N,i}]^2 \Gamma_i^s + 1 / \bar{\gamma}_1}} \right], \quad (10)$$

where  $\Gamma_i = E\{C_i(k) - \hat{C}_i(k)\} / E\{C_i(k)\}^2 = E\{e_i(k)\}^2$  is the normalized channel estimation error variance of user  $i$  (with normalization  $E\{C_i(k)\}^2 = 1$  as described in

Section 2), and  $\bar{\gamma}_1 = E\{C_1(k)\}^2 Eb_1 / N_0 = Eb_1 / N_0$  is the average SNR of user 1. The performance of the 2S and the DF detectors are limited not only by the channel estimation error of the desired user (user 1), but also by the channel estimation errors of other users. This fact is more obvious when we investigate the signal of the desired user (user 1) at the output of the second stage of a 2S detector after MAI cancellation (assuming that other users have correct decisions):

$$\begin{aligned} \mathfrak{z}_1'(k) &= \sqrt{Eb_1} C_1(k) b_1(k) \\ &+ \sum_{i=2}^N \sqrt{Eb_i} \mathbf{R}_{1,i} [C_i(k) - \hat{C}_i(k)] b_i(k) + n_1(k). \end{aligned} \quad (11)$$

The summation term in (11) is the residual interference due to imperfect estimation of the channel coefficient of other users.

The estimation error is found to be irreducible and it converges to the power of the driving noise of a fading channel (the second order AR process) as SNR increases [8]. The irreducible channel estimation errors result in error floors for all the detectors.

#### 5. Numerical Examples

Both analytical and simulation results are presented in the following numerical examples. The parameters are chosen as follows: for the fading channel model, the radius of the poles of (4)  $r_d = 0.998$  is used to reflect the peaks in the power spectrum, the maximum Doppler frequency  $f_d = 80$  Hz corresponds to vehicle speed of 60 miles per hour, and the data rate ( $1/T_s$ ) is 10 Kbps. The resulting parameters of the second order AR process are  $a_1 = -1.99348$  and  $a_2 = 0.996$ .

The cross-correlation for the 2-user scenario is 0.9, and the cross-correlation matrices  $\mathbf{R}$  for 4-user and 24-user cases are derived from Gold sequence of length 7 and 31 respectively. In particular, for the case of 24 users, we choose 24 Gold sequences of length 31, and cyclically shift each sequence by +1 chip or -1 chip. The purpose is to account for the effect of imperfect chip-level synchronization, and to mimic the asynchronous CDMA channel. With such arrangement, the off diagonal element will have one of the three values  $\{-1/31, -9/31, 7/31\}$ .

Figures 2-4 show the results of 2-user, 4-user, and 24-user scenarios in which all users have the same average SNR. In these plots, lines represent the analytical results ((8)-(10)) and points (circles, crosses, and plus signs) are the simulation results. The BERs of the 2S and the DF are almost the same and only the results of the 2S are shown here. First, we observe several error floors: the

decorrelator with DPSK has the highest error floor with the limiting error rate around  $10^{-3}$ , and the multiuser detectors with DC-PSK have lower error floors. The former error floor is due to the normalized fading rate (the product to the Doppler frequency and the sampling period) while the latter ones are due to the irreducible channel estimation errors. We also observe the cross-over between the decorrelator and the 2S. The cross-over SNR can be found by comparing (8) and (9) with the value of  $\Gamma_1$  from Ricatti equation [5] and it satisfies

$$\sum_{i=2}^N (Eb_i/Eb_1) [\mathbf{R}_{1,i}]^2 \Gamma_i + (1 - [\mathbf{R}^{-1}]_{1,1})/\bar{\gamma}_1 = 0. \quad (12)$$

For the 2-user scenario, with the same average SNR for both users ( $Eb_1 = Eb_2$ , or  $\bar{\gamma}_1 = \bar{\gamma}_2$ ), the cross-over point is around 40 dB. This indicates that beyond this SNR, the more complicated multiuser detectors--the 2S and the DF, actually perform worse than the simpler decorrelator. The 4-user and the 24-user scenarios shown in Figures 3 and 4 also confirm this observation.

It is noted that for a single user system, the limiting value of the normalized error variance,  $\Gamma$ , is the same as that of a decorrelator. Therefore, they have the same error floor, i.e., their performance is asymptotically the same. On the other hand, the limiting BER of the 2S and the DF is higher than that of a single user system because of the contribution of other users' estimation error ( $\sum_{i=2}^N (Eb_i/Eb_1) [\mathbf{R}_{1,i}]^2 \Gamma_i$  in (9)). This result is quite different from the case of the perfect channel estimation in which the performance of the 2S and the DF asymptotically approaches that of a single user system [13]. Further comparison with the case of perfect channel estimation shows that the performance gain of the 2S and the DF over the decorrelator is not as significant when channel is mismatched.

We also investigate near-far scenarios for 4 users and 24 users, shown in Figures 5 and 6. When the interferers are stronger than the desired user (user 1) by 6 dB, we find that the performance of the 2S and the DF degrades compared with the case of equal strength (see Figure 3 and 5, 4 and 6). This is again a different result when compared with the perfect channel estimation case [13]. For the perfect channel estimation case, in the near-far scenario, decisions of interferers in the 2S and the DF are more reliable and the MAI cancellation is more complete than in the case of equal strength. Therefore, the 2S and the DF are closer to the single user bound when interferers are stronger than in the case of equal strength. In the channel mismatched condition, the residual interference (summation in (11)) is the dominant factor of the performance of the 2S and the DF for high SNR. In the near-far scenario, the residual interference is greater than that of the equal strength case, and therefore the 2S and the DF perform worse in the near-far scenario. This is due to the following reason. Although in the near-far scenario the estimation errors  $\Gamma_i$  of other users are reduced compared with those of the equal strength case, the total power of the resultant residual interference

$\sum_{i=2}^N (Eb_i/Eb_1) [\mathbf{R}_{1,i}]^2 \Gamma_i$  is greater than that of the equal strength case due to higher power ratios ( $Eb_i/Eb_1$ ). The

performance degradation of the 2S and the DF in the near-far scenario is more obvious in high SNR since the estimation error converges to the limiting value  $\Gamma_i$  and can not be further reduced.

The analysis and the simulation results for these examples indicate that the decorrelator is more robust than the 2S and the DF in the presence of the channel mismatch.

## 6. Conclusion and Future Work

We showed that the burst error problems due to the phase reversal in decision-directed Kalman channel estimator can be solved by encoding data bits differentially. With differential encoding, the performance of multiuser detectors with Kalman channel estimators is analyzed and verified by simulations. We observe that performance of considered multiuser detectors is similar. The performance gain of more complex detectors (the 2S and the DF) is only observed in the low SNR region, and is not as significant as in the case of perfect channel estimation. In high SNR region, the residual interference of the these two detectors caused by channel mismatch becomes large enough to degrade their performance whereas the decorrelator tends to the single user bound in this case. Thus, in the case of channel mismatch, the estimation error, not MAI, limits the performance of multiuser detectors. The fact that the residual interference is larger in the near-far scenario than that of the equal strength case causes greater performance degradation of the 2S and the DF in near-far scenario. Both analytical and simulation results show that the simpler decorrelator is more robust than more complex 2S and DF multiuser detectors in the presence of channel mismatch. Future work will concentrate on performance evaluation of multiuser detectors with channel estimators using Jakes fading channel model [14]. We will also compare performance of multiuser detectors investigated in this paper with the successive interference cancellation scheme [4].

## References

- [1] R. Lupas, S. Verdu, "Linear Multiuser Detectors for Synchronous Code-Division Multiple-Access Channel," *IEEE Transactions on Information Theory*, Vol. IT-35, No. 1, Jan. 1989, pp. 123-136.
- [2] M.K. Varanasi, B. Aazhang, "Near-optimum Detection in Synchronous Code-Division Multiple Access Channel," *IEEE Transactions on Communications*, Vol. COM-39, No. 5, May 1991, pp. 725-736.
- [3] A. Duel-Hallen, "Decorrelating Decision-Feedback Multiuser Detector for Synchronous Code-Division Multiple Access Channel," *IEEE Transactions on Communications*, Vol. COM-41, No. 2, Feb. 1993, pp. 285-290.
- [4] P. Patel, J. Holtzman, "Analysis of a Simple Successive Interference Cancellation Scheme in DS/CDMA System," *IEEE JSAC - Special issue on CDMA*, Vol. 12, No. 5, June 1994, pp. 796-807.

- [5] B.D.O. Anderson and J.R. Moore, *Optimal Filtering*, Prentice-Hall, 1979.
- [6] L. Lindbom, "Simplified Kalman Estimation of Fading Mobile Radio Channels: High Performance at LMS Computational Load," *IEEE ICASSP*, Vol. 3, April 1993, pp. 352-355.
- [7] Z. Zvonar, M. Stojanovic, "Performance of Multiuser Diversity Reception in Nonselective Rayleigh Fading CDMA Channels," *Proceedings of IEEE GLOBECOM CTMC*, San Francisco, Nov. 28-Dec. 2, 1994, pp. 171-175.
- [8] H.Y. Wu, A. Duel-Hallen, "Performance Comparison of Multiuser Detectors with Channel Estimation for Flat Rayleigh Fading CDMA Channels," to appear in *Wireless Personal Communications, Special Issue on "Interference in Mobile Wireless Systems,"* Kluwer.
- [9] H.Y. Wu, A. Duel-Hallen, "Channel Estimation and Multiuser Detection for Frequency-Nonselective Fading Synchronous CDMA Channel," *Proc. of Thirty-Second Annual Allerton Conference on Communication, Control and Computing*, Monticello, Sept. 1994, pp. 335-344.
- [10] R. Haeb, H. Meyr, "A Systematic Approach to Carrier Recovery and Detection of Digitally Phase Modulated Signals on Fading Channels," *IEEE Transactions on Communications*, Vol. 37, No. 7, July 1989, pp. 748-754.
- [11] J.G. Proakis, *Digital Communications*, McGraw Hill, 1989.
- [12] M. Varanasi, "Noncoherent Detection in Asynchronous Multiuser Channels," *IEEE Transactions on Information Theory*, Vol. IT-39, No. 1, Jan. 1993, pp. 156-176.
- [13] H.-Y. Wu, A. Duel-Hallen, "Performance of Multiuser Decision Feedback Detector for Flat Rayleigh Fading Synchronous CDMA channel," *The Proceedings of the 28th Annual Conference on Information Science and Systems*, Princeton, New Jersey, March 16-18, 1994, pp. 133-138.
- [14] W.C. Jakes, Jr., *Microwave Mobile Communication*, John Wiley & Sons, New York, 1974, p. 75.

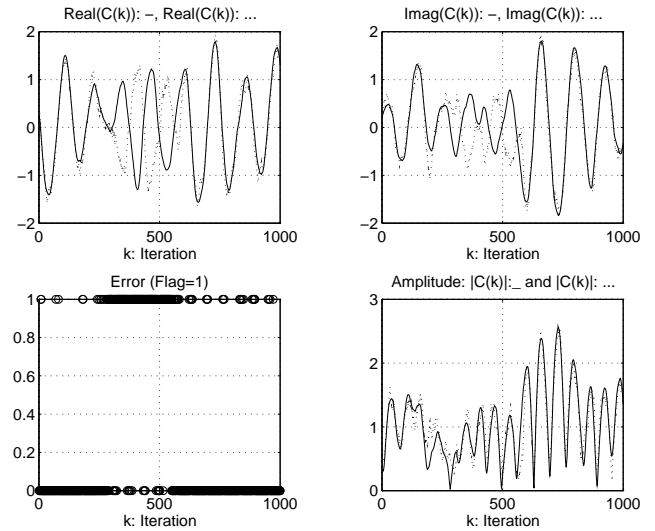


Figure 1

Reversal Phenomenon

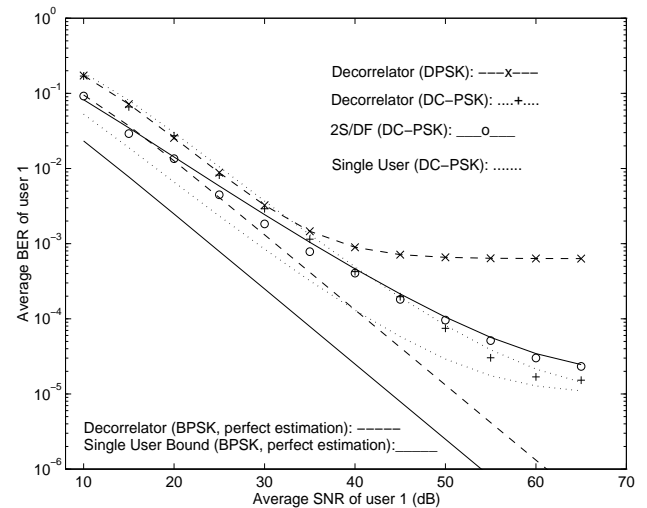


Figure 2

Performance of multiuser detectors for a 2-user mismatched CDMA channel with equal average strength

$$\bar{\gamma}_1 = \bar{\gamma}_2 \text{ and cross-correlation matrix } \mathbf{R} = \begin{bmatrix} 1 & 0.9 \\ 0.9 & 1 \end{bmatrix}$$

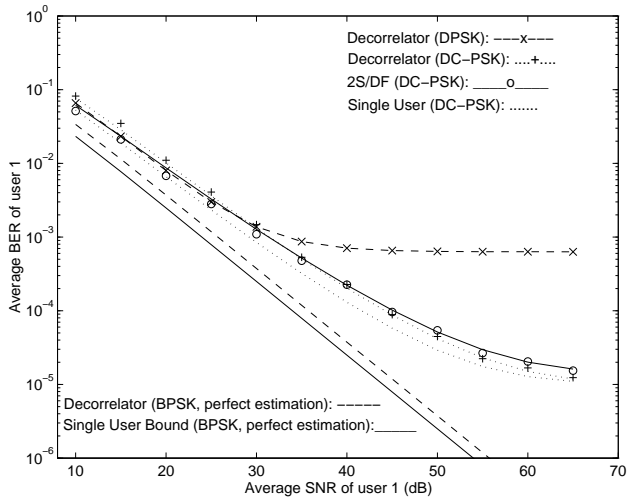


Figure 3

Performance of multiuser detectors for a 4-user mismatched CDMA channel with equal average strength  $\bar{\gamma}_i = \bar{\gamma}_1$  ( $i = 2, 3, 4$ ) and cross-correlation matrix

$$\mathbf{R} = \frac{1}{7} \begin{bmatrix} 7 & -1 & 3 & 3 \\ -1 & 7 & 3 & -1 \\ 3 & 3 & 7 & -1 \\ 3 & -1 & -1 & 7 \end{bmatrix}$$

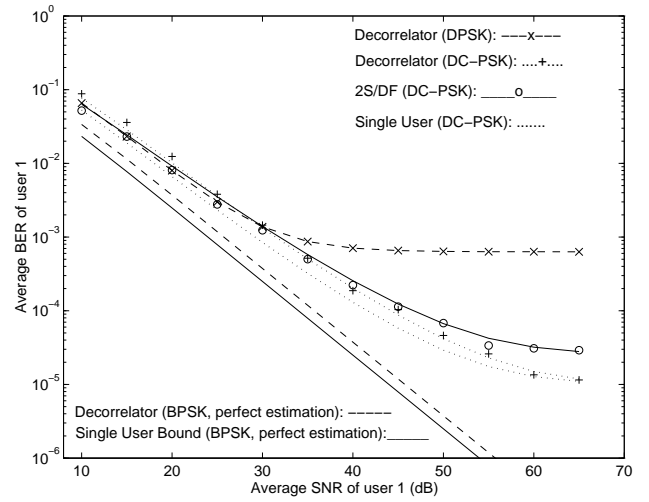


Figure 5

Performance of multiuser detectors for a 4-user mismatched CDMA channel with unequal average strength  $\bar{\gamma}_i = 4 \bar{\gamma}_1$  ( $i = 2, 3, 4$ ) (near-far) and cross-correlation matrix

$$\mathbf{R} = \frac{1}{7} \begin{bmatrix} 7 & -1 & 3 & 3 \\ -1 & 7 & 3 & -1 \\ 3 & 3 & 7 & -1 \\ 3 & -1 & -1 & 7 \end{bmatrix}$$

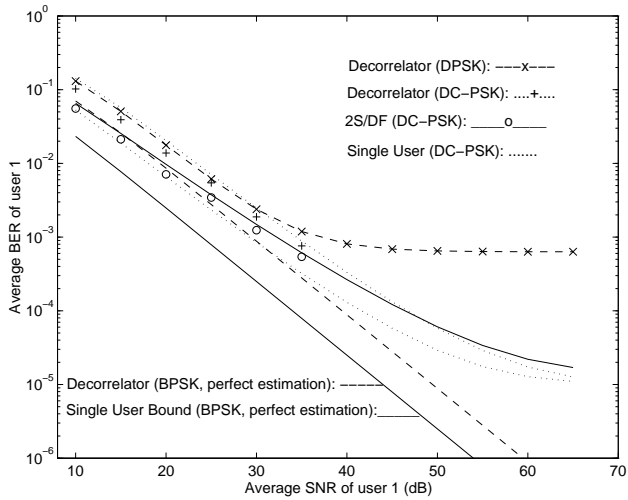


Figure 4

Performance of multiuser detectors for a 24-user mismatched CDMA channel with equal average strength  $\bar{\gamma}_i = \bar{\gamma}_1$  ( $i = 2, \dots, 24$ )

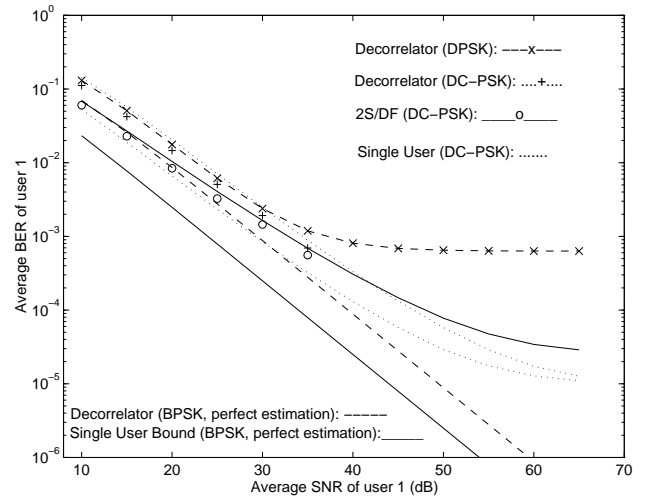


Figure 6

Performance of multiuser detectors for a 24-user mismatched CDMA channel with unequal average strength  $\bar{\gamma}_i = 4 \bar{\gamma}_1$  ( $i = 2, \dots, 24$ ) (near-far)